

# Fast calculation of best focus position

Vitalii Bezzubik<sup>\*a</sup>, Nickolai Belashenkov<sup>a</sup>, Gleb Vdovin<sup>a,b,c</sup>

<sup>a</sup>ITMO University, Kronverksky pr. 49, St.Petersburg, Russian Federation, 197101,

<sup>b</sup>Delft University of Technology, DCSC, 2628 CD, Delft, the Netherlands,

<sup>c</sup>Flexible Optical B.V., Polakweg 10-11, 2288 GG Rijswijk, the Netherlands.

## ABSTRACT

New computational technique based on linear-scale differential analysis (LSDA) of digital image is proposed to find the best focus position in digital microscopy by means of defocus estimation in two near-focal positions only. The method is based on the calculation of local gradients of the image on different scales using its convolution with a number of differential filters of linearly varying sizes, consequent removal of noisy pixels out of consideration, and selection of pixels at the edges of objects. It is shown that the mean values of the selected gradients decrease while the scale increases thus the rate of change of these mean values of gradients unambiguously determines the magnitude of digital image defocus as a function of scale. Using this method the value and sign of defocus can be found if the result of LSDA of captured images is compared with pre-defined look-up table. The robustness of the proposed method to spatial noise is achieved by ignoring pixels that are corrupted by spatial noise within the areas of the image outside the edges of objects. Most computational operations of the method are based on integer arithmetic that simplifies its practical implementation and significantly improves the performance. The latter aspect is particularly important for practical use in real-time imaging systems.

**Keywords:** Digital image, defocus blur, autofocus, local differential response, histogram of gradients.

## 1. INTRODUCTION

The most known algorithms for search of the best focus position of imaging system are based on consequent measuring of the estimation function in different positions of lens and determination of the extremal value of this function [1-3]. However such technique in practice is insufficiently effective because it requires several iterations and takes a long time to provide mechanical movements of lens before the best focal position is found. Recently the method of phase search [4-5] has been proposed and realized. It provides faster technique however it has a significant drawback of layout complexity and high cost of the imaging system. Therefore the perspectives of application of this technique are limited. The development of fast and cost-effective method of search for the best focus position with minimum measurements of the estimation function is of current interest.

Basic principles of blur estimation to be taken in consideration as guidelines for fast algorithm of best focus position search have been published in [6-10]. In present paper we propose a method of best focus position search which is based on linear-scale differential analysis (LSDA) of digital image. This technique combines the advantages of high-speed performance and reduced sensitivity to spatial noise.

Thus formation of resulting image intensity distribution  $g(x, y)$  on digital sensor of imaging system may be described as a convolution of non-distorted image intensity function  $f(x, y)$  with kernel  $h(x, y)$  and additive spatial noise  $n(x, y)$ :

$$g(x, y) = f(x, y) \otimes h(x, y) + n(x, y), \quad (1)$$

where  $x, y$  – spatial coordinates in the image plane,  $\otimes$  means the convolution operation,  $h(x, y)$  - kernel of distortion including irremovable aberrations of optical system and defocusing. In present work we do not separate the kernel  $h(x, y)$  according to physical factors because it is not important for given task. The position of best focus should be found as the position of the lens providing the highest sharpness of the image wherein the knowledge of the kernel is out of interest.

\*Vitalii Bezzubik: bezzubik@mail.ru

Three-Dimensional and Multidimensional Microscopy: Image Acquisition and Processing XXII, edited by  
Thomas G. Brown, Carol J. Cogswell, Tony Wilson, Proc. of SPIE Vol. 9330, 93300W · © 2015 SPIE  
CCC code: 1605-7422/15/\$18 · doi: 10.1117/12.2080965

Proc. of SPIE Vol. 9330 93300W-1

## 2. LINEAR-SCALE DIFFERENTIAL ANALYSIS

In [11] the method of digital image deblurring based on linear-scale differential analysis (LSDA) has been proposed. In present paper the same analysis is used to evaluate the image blur which is the measure of imaging system defocus. Let's recall the basic principles of linear multi-scale analysis. Let's consider digital gray-scale image  $f_{i,j}$  having width  $M$  (x-coordinate, index  $i$ ) and height  $N$  (y-coordinate, index  $j$ ) pixels as a source. Assume that defocused image  $g_{i,j}$  may be represented as a result of convolution of  $f_{i,j}$  with a blur kernel  $h_{p,q}$ . Then the image on sensor will be described as:

$$g_{i,j} = \sum_p \sum_q f_{i+p,j+q} \cdot h_{p,q} \quad (2)$$

Assume that  $g_{i,j} = f_{i,j} \quad \forall i,j$  and no blur occurs if the optical system provides the best focus position.

Let's consider a number of square digital filters separately for  $x$  and  $y$  coordinates, with odd number of rows and columns  $S \times S$  ( $S \geq 3$ ) in the form:

$$Kx_{p,q}^{(S)} = \begin{cases} -1, & -S_c \leq p < 0, & -S_c \leq q \leq S_c \\ 0, & p = 0, & -S_c \leq q \leq S_c \\ +1, & 0 < p \leq S_c, & -S_c \leq q \leq S_c \end{cases}, \quad Ky_{p,q}^{(S)} = \begin{cases} -1, & -S_c \leq p \leq S_c, & -S_c \leq q < 0 \\ 0, & -S_c \leq p \leq S_c, & q = 0 \\ +1, & -S_c \leq p \leq S_c, & 0 < q \leq S_c \end{cases} \quad (3)$$

where  $S_c = (S-1)/2$ ,  $p$  and  $q$  – indices on  $x$  and  $y$  coordinates, respectively. These indices change within the range from  $-S_c$  to  $S_c$ . Further we will call  $S$  as “scale” similar to the definition used in wavelet-analysis. The examples of two digital filters of  $S=3$  and  $S=5$  scales are given below:

$$Kx^{(3)} = \begin{vmatrix} -1 & 0 & +1 \\ -1 & 0 & +1 \\ -1 & 0 & +1 \end{vmatrix}, \quad Ky^{(3)} = \begin{vmatrix} -1 & -1 & -1 \\ 0 & 0 & 0 \\ +1 & +1 & +1 \end{vmatrix}, \quad Kx^{(5)} = \begin{vmatrix} -1 & -1 & 0 & +1 & +1 \\ -1 & -1 & 0 & +1 & +1 \\ -1 & -1 & 0 & +1 & +1 \\ -1 & -1 & 0 & +1 & +1 \\ -1 & -1 & 0 & +1 & +1 \end{vmatrix}, \quad Ky^{(5)} = \begin{vmatrix} -1 & -1 & -1 & -1 & -1 \\ -1 & -1 & -1 & -1 & -1 \\ 0 & 0 & 0 & 0 & 0 \\ +1 & +1 & +1 & +1 & +1 \\ +1 & +1 & +1 & +1 & +1 \end{vmatrix} \quad (4)$$

It should be noted that  $Kx^{(3)}$  and  $Ky^{(3)}$  in (4) represent the well-known Prewitt filters which are widely used for edge detection in digital image processing. As it has been shown in [11] filters  $Kx^{(5)}$  and  $Ky^{(5)}$  and following ( $S>5$ ) ones allow to reduce the influence of noise because of their averaging properties. This noise-dumping property becomes better as scale  $S$  grows, however it results in a loss of fine details of the image. The set of filters (3) satisfy the conditions:

$$\sum_{p=-S_c}^{S_c} \sum_{q=-S_c}^{S_c} Kx_{p,q}^{(S)} = 0, \quad \sum_{p=-S_c}^{S_c} \sum_{q=-S_c}^{S_c} Ky_{p,q}^{(S)} = 0.$$

Using sequent discrete convolution of source image  $g_{i,j}$  with the filters (3) under different scales we get the arrays  $Rx_{i,j}^{(S)}$  and  $Ry_{i,j}^{(S)}$ :

$$Rx_{i,j}^{(S)} = A^{-1}(S) \sum_{p=-S_c}^{p=S_c} \sum_{q=-S_c}^{q=S_c} g_{i+p,j+q} \cdot Kx_{p,q}^{(S)} \quad (5)$$

$$Ry_{i,j}^{(S)} = A^{-1}(S) \sum_{p=-S_c}^{p=S_c} \sum_{q=-S_c}^{q=S_c} g_{i+p,j+q} \cdot Ky_{p,q}^{(S)}, \quad (6)$$

which we'll call normalized differential responses in the point with coordinates  $(i, j)$  along the correspondent coordinate in definite scale  $S$ . In expressions (5) and (6) the normalizing coefficient  $A(S)$  is equal to  $S(S^2 - 1)/4$ .  $A(S)$  is defined in this way to provide the equality of absolute values of integral differential responses  $C_x$  and  $C_y$  for any scale  $S$  for the whole image:

$$\sum_{i,j} |R_{x_{i,j}}^{(S)}| = C_x = \text{const} \forall S, \quad \sum_{i,j} |R_{y_{i,j}}^{(S)}| = C_y = \text{const} \forall S. \quad (7)$$

It should be noticed that local values of  $C_x$  and  $C_y$  calculated in the vicinity of the edge of the object are equal to the difference of intensity of source image in this neighborhood location for any scale  $S$ .

Then we need to find the arrays of gradients in corresponding scales:

$$R_{i,j}^{(S)} = \sqrt{\left(R_{x_{i,j}}^{(S)}\right)^2 + \left(R_{y_{i,j}}^{(S)}\right)^2}. \quad (8)$$

As it is mentioned above for scale  $S=3$  filters  $K_x^{(3)}$  and  $K_y^{(3)}$  are the Prewitt filters so the value  $R_{i,j}^{(3)}$  is obviously the local gradient. For scales  $S \geq 5$  the values  $R_{i,j}^{(S)}$  are the gradients averaged across the local area thus said area is defined by the sizes of filters  $K_x^{(S)}$  and  $K_y^{(S)}$ .

### 3. DEFOCUS BLUR ESTIMATION

The algorithm of evaluation of the defocus of an optical system is tested on three examples of simplified test images. We assume that defocus blur kernel  $h_{i,j}$  is Gaussian with parameter  $\sigma$ . First test image represents a sharp step edge of 100 to 200 units of grey-level intensity, the second one is the same edge blurred by Gaussian kernel with  $\sigma = 2$  and the third one is a solitary single noisy pixel of 100 units of grey-level intensity on a uniform background (grey level 100). The profiles of these images along  $x$  direction are represented in Figure 1 (top row). Applying linear multi-scale analysis to the test images, one can calculate, using (5) and (6), the normalized differential responses  $R_{x_{i,j}}^{(S)}$  and  $R_{y_{i,j}}^{(S)}$ . The results of calculation of normalized differential responses  $R_{x_{i,j}}^{(S)}$  along  $x$  coordinate for three types of images direction are represented in Figure 1. In Figure 1-A top view shows the profile of intensity of source image as a sharp step edge. From top to bottom the profiles of normalized differential responses  $R_{x_{i,j}}^{(S)}$  for four lowest scales ( $S=3, 5, 7$  and  $9$ ) are shown. In Figures 1-B and 1-C the same illustrations are represented for blurred ( $\sigma = 2$ ) step edge and single noise intensity fluctuation on uniform background, respectively.

As it has been noted in [11] that the pixels corresponding to maxima of absolute values  $R_{x_{i,j}}^{(S)}$  and  $R_{y_{i,j}}^{(S)}$  are found at the edges of the objects. In order to find these pixels it is necessary to calculate auxiliary arrays of derivatives of differential responses on corresponding coordinates and scales:

$$P_{x_{i,j}}^{(S)} = \frac{1}{2} \left( R_{x_{i+1,j}}^{(S)} - R_{x_{i-1,j}}^{(S)} \right), \quad P_{y_{i,j}}^{(S)} = \frac{1}{2} \left( R_{y_{i,j+1}}^{(S)} - R_{y_{i,j-1}}^{(S)} \right). \quad (9)$$

Any pixel with coordinates  $(i, j)$  we mark as a pixel lying at the edge if:

$$\begin{cases} P_{x_{i-1,j}}^{(S)} \cdot P_{x_{i+1,j}}^{(S)} < 0, \text{ for } |R_{x_{i,j}}^{(S)}| \geq |R_{y_{i,j}}^{(S)}| \\ P_{x_{i,j-1}}^{(S)} \cdot P_{x_{i,j+1}}^{(S)} < 0, \text{ for } |R_{x_{i,j}}^{(S)}| < |R_{y_{i,j}}^{(S)}| \end{cases}. \quad (10)$$

This expression means that at the first stage of consideration the direction having the higher absolute value of differential response should be found and then the analysis of derivative signs in neighboring pixels is carried out along the

corresponding direction. If derivative changes its sign the corresponding product in (10) becomes negative. Hence the pixel with coordinates  $(i, j)$  can be defined as a point of local gradient maximum. Below, the values of these maxima we denote as  $Rm_{i,j}^{(S)}$ . It should be mentioned that the rule (10) produces points of local gradient maxima in pairs, because the sets of filters (3) produce conjugated symmetrical values of differential responses at opposite sides of the edge.

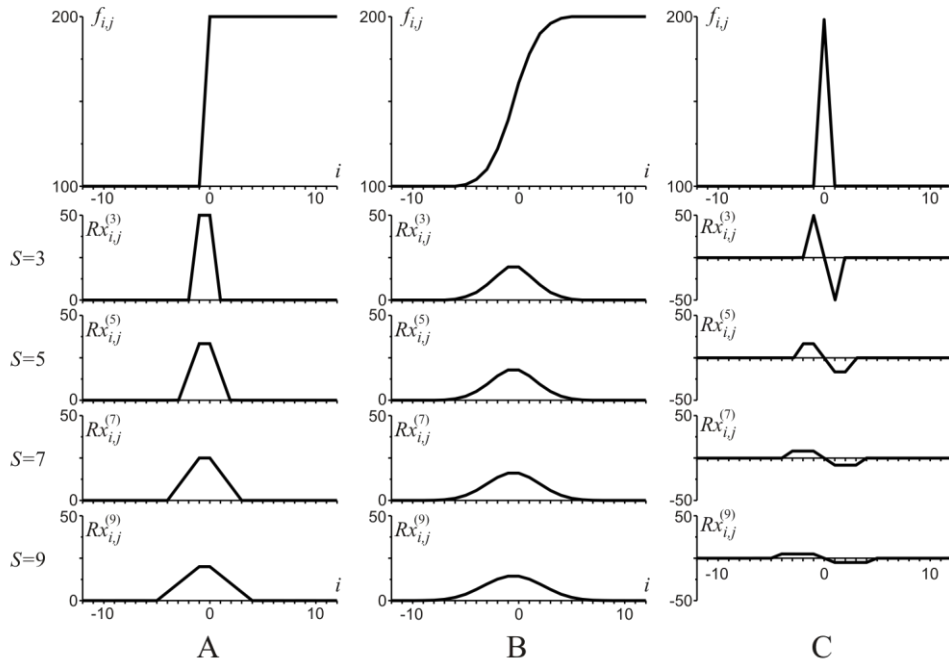


Figure 1. Normalized differential responses  $R_{i,j}^{(S)}$  in four lowest scales  $S$ .  
 A – sharp step edge, B – blurred step edge, C – single noisy pixel.

Figure 2 shows that maxima values of intensity gradients  $Rm_{i,j}^{(S)}$  decrease if scale  $S$  grows both for sharp and blurred step edges. The same dependence is demonstrated for a single noisy pixel. The scale-fading is stronger for sharp edge ( $Rm_{i,j}^{(9)} = 0.4Rm_{i,j}^{(3)}$ , see Figure 2-A) and weaker for blurred edge ( $Rm_{i,j}^{(9)} = 0.75Rm_{i,j}^{(3)}$ , see Figure 2-B) the scale-fading of  $Rm_{i,j}^{(S)}$  depends on blur parameter. It is stronger for sharper step edges. This property of filters (3) allows to define a method of search for the best focus.

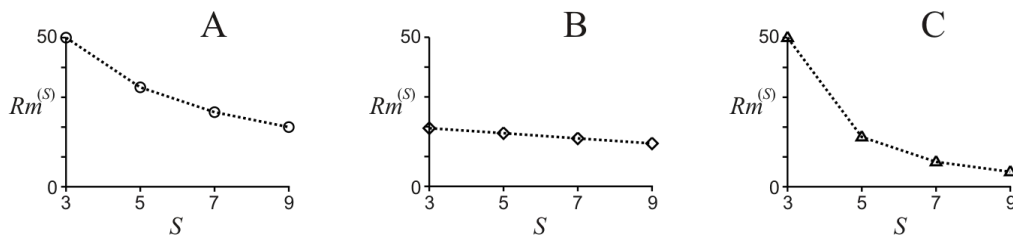


Figure 2. Scale-fading of  $Rm^{(S)}$ .  
 A – sharp step edge, B – blurred step edge, C – single noisy pixel.

The scale-fading of  $Rm_{i,j}^{(S)}$  in the vicinity of noise pixels on a uniform background should be considered separately. Figure 2-C shows that  $Rm_{i,j}^{(S)}$  value for single noisy pixel decreases rapidly ( $Rm_{i,j}^{(9)} = 0.1Rm_{i,j}^{(3)}$ ) due to averaging properties of filters (3). This advantage allows to suppress the contribution of additive noise.

Figures 1, 2 illustrate 1-D profiles of gradients only. In the 2-D case it is convenient to use histograms of gradients in different scales, calculated according to (8). If blurred step edge (Figure 1-B) is used as a test image, then histograms of gradients in four lowest scales can be represented as shown in Figure 3 row A. Here the calculation of histograms have been made using a moderate-size window. Besides, the null values of gradients are excluded. The number of peaks in histograms grows with scale  $S$ . After selection of pixels lying on the object's edges using (10), the histograms of gradients  $Rm^{(S)}$  in four lowest scales may be represented as follows (see Figure 3 row B).

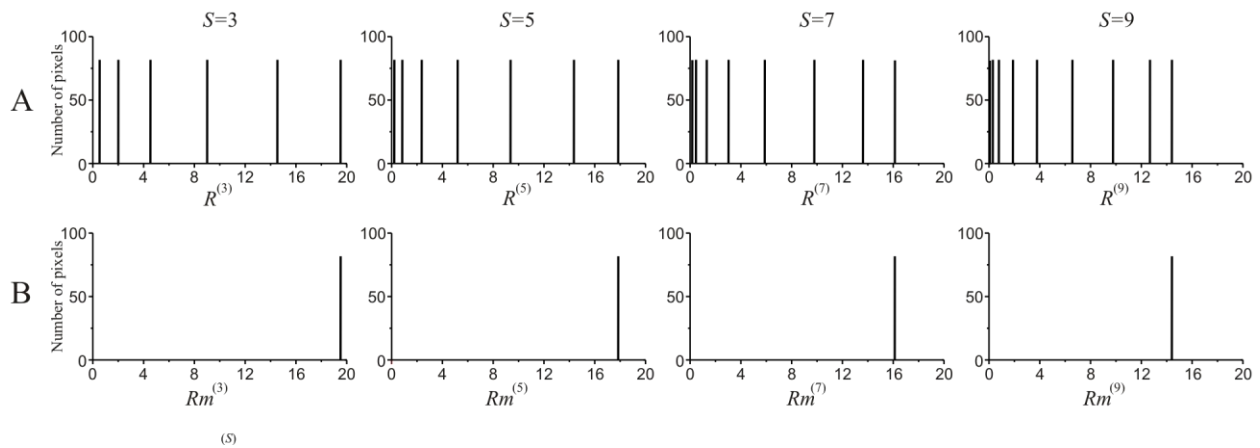


Figure 3. Histograms of intensity gradients of blurred ( $\sigma = 2$ ) step edge (A) and maxima values of intensity gradients (B).

The presented histograms correspond to single blurred edge of definite contrast. In the case of image comprising a large number of blurred objects having different contrasts, the histograms of gradient's maxima have a lot of peaks of different height even when no noise is applied to the image. It is impossible to analyze the scale-fading of a separate gradient's maximum. That's why it is necessary to use the mean values averaged across the whole image. Here we introduce the gradient mean value  $\bar{R}^{(S)}$  and gradient's maxima mean value  $\bar{R}m^{(S)}$  in different scales  $S$  :

$$\bar{R}^{(S)} = (MN)^{-1} \sum_i^M \sum_j^N R_{i,j}^{(S)}, \quad (11a)$$

$$\bar{R}m^{(S)} = (MN)^{-1} \sum_i^M \sum_j^N Rm_{i,j}^{(S)}, \quad (11b)$$

and scale-fading indices of  $\bar{R}m^{(S)}$  :

$$B^{(S)} = \frac{\bar{R}m^{(S)}}{\bar{R}m^{(3)}}. \quad (12)$$

It is evident that the  $B^{(3)} = 1$ . In Figure 4-A the values of  $B^{(S)}$  are represented for sharp step image ( $\sigma = 0$ ) and blurred step images. One can see that decrease of scale-fading values  $B^{(S)}$  depend on the blur value. It is high for sharp step image and becomes lower with defocus.

Defocus of the image may be evaluated definitely under consideration of  $B^{(5)}$  or  $B^{(7)}$ . In Figure 4-B the dependences of these indices on the parameter of Gaussian blur kernel is represented for step image. The blur parameter (defocus

measure) can be evaluated if  $B^{(5)}$  or  $B^{(7)}$  values are known. In order to determine the sign of defocus it is necessary to repeat the calculation of  $B^{(5)}$  or  $B^{(7)}$  in different focal position of imaging system.

The proposed method can be applied for any imaging system if the lookup table with focal position data corresponding to the calculated focus measure is preliminary filled.

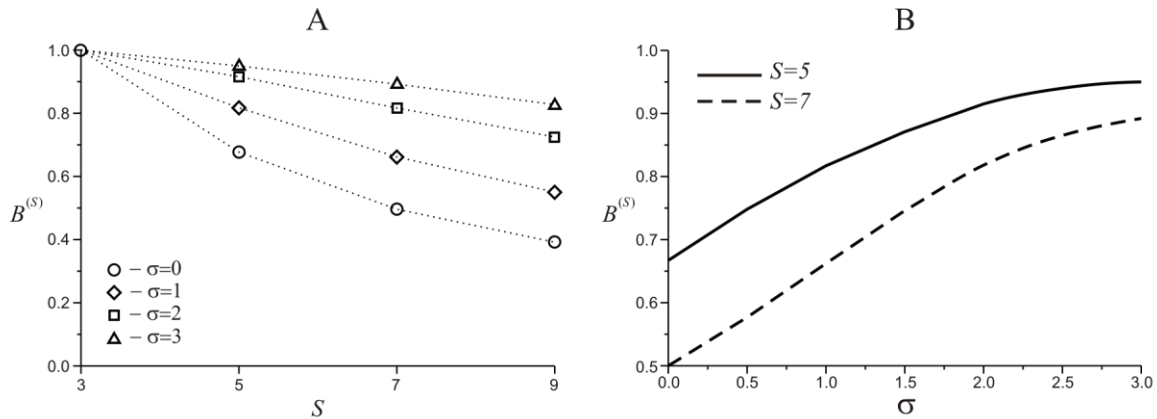


Figure 4. Scale-fading indices (A) and dependences of  $B^{(5)}$  and  $B^{(7)}$  on blur parameter (B).

#### 4. NOISE REJECTION

In practice, digital images are often corrupted by the spatial noise. This noise influences the stability of image processing, including the algorithm of best focal position search. It is important to test the proposed method for noise images. Below we describe how it is possible to make the proposed method more stable and less sensitive to the spatial noise.

In [12] it has been shown that intensity gradients of noisy image calculated with the help of low-scale differential filters have Rayleigh distribution. For LSDA this distribution can be defined as:

$$H(R^{(S)}, a^{(S)}) = (a^{(S)})^{-2} R^{(S)} \exp\left\{-\left(\frac{[R^{(S)}]^2}{2[a^{(S)}]^2}\right)\right\}. \quad (13)$$

where  $a^{(S)}$  is the standard deviation of Rayleigh distribution in the  $S$  scale.

In present work the intensity gradients are calculated in different scales. For each scale  $S$  these gradients are distributed with definite standard deviation  $a^{(S)}$  thus the ratio of distribution widths of noisy gradients and gradients calculated in pixels at object's edges decreases while scale  $S$  grows.

In Figure 5-A the histograms of gradients of blurred image ( $\sigma = 2$ ) corrupted by the Gaussian noise with standard deviation equal to 0,01 are represented. One can see from Figure 3-A and Figure 5-A that even low spatial noise influences considerably on the histograms of intensity gradients in all scales. In the low scales this influence is more apparent: low values of true image gradients become invisible under high noisy gradients. However Figure 5-A shows that in high scales the portion of true image gradients masked by noisy gradients decreases while scale  $S$  grows. Those gradients which correspond to pixels at object's edge become larger due to adding of values of noisy gradients. This results in "expanding" of gradient's peaks in accordance with Rice distribution:

$$H(R^{(S)}, a^{(S)}, \xi) = (a^{(S)})^{-2} R^{(S)} \exp\left\{-\left(\frac{[R^{(S)}]^2 + \xi^2}{2[a^{(S)}]^2}\right)\right\} \cdot I_0\left(R^{(S)}[a^{(S)}]^{-2}\right). \quad (14)$$

where  $\xi$  - mean value of intensity gradient for definite object's edge.

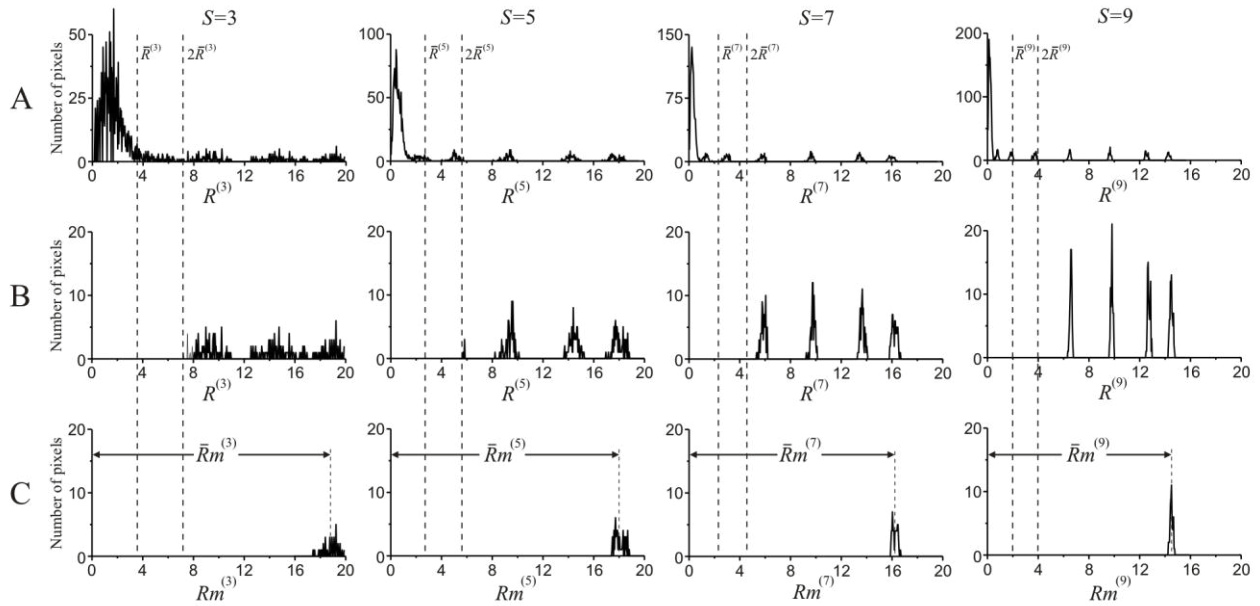


Figure 5. Histograms of intensity gradients of blurred ( $\sigma = 2$ ) and noisy step edge before (A) and after (B) rejection of noisy gradients. Maxima values of intensity gradients (C).

The rejection of noisy gradients is absolutely necessary otherwise the calculation of derivatives of intensity gradients using (9) will produce false zero-crossings and rule (10) will produce a lot of false points of local gradient maxima. Therefore we suggest to make the following steps of algorithm illustrated by flowchart in figure 6:

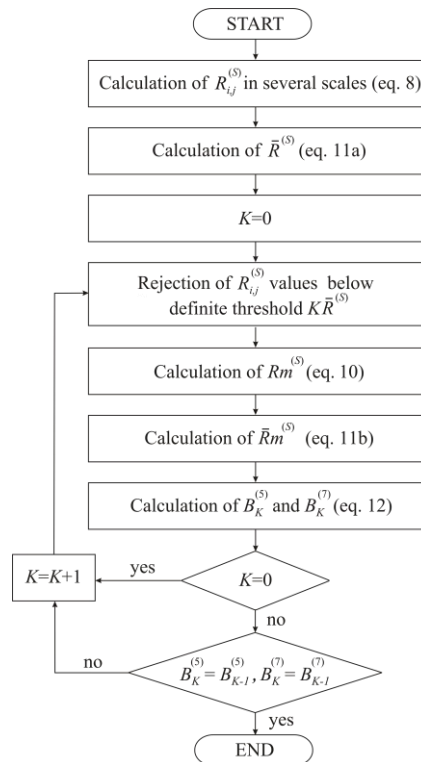


Figure 6. Flowchart of proposed algorithm.

In Figure 5 row B the histograms of intensity gradients obtained with a threshold at  $K=2$  in accordance to the flowchart (Figure 6) are shown. In Figure 5 row C the histograms of intensity gradients after calculation of  $Rm^{(S)}$  and  $\bar{R}m^{(S)}$  are represented.

## 5. REMARKS

In conclusion, some important recommendations for practical implementation of the proposed method should be done. First of all, it should be noticed that scale-fading indices in Figure 4-A do not depend on image content if the object's edges in this image are isolated. If the edges of different objects intersect, the proposed method requires an additional procedure of rejection. This rejection should be applied to those gradients which are calculated in pixels lying at the low contrast edges. Said rejection may be done similarly to noise rejection technique described in Chapter 4. If no rejection applied, false zero-crossings can change the values of scale-fading indices in Figure 4-A. That inevitably results in errors of  $B^{(5)}$  and  $B^{(7)}$  values.

The proposed method is expected to be effective in microscopes, when the blur parameter is uniform across the field. Nevertheless, the method can be used in any imaging system, even with different blur parameters across the image. In this case it is advisable to select a regions of interest with a constant blur.

It is evident that the level of spatial noise influences the effectiveness and accuracy of the proposed method. High level of noise in the image results in the distortion of the distribution of intensity gradients on a uniform background, especially in the scale with  $S=3$ , and makes thresholding procedure much more difficult. In this case, the algorithm of the proposed method can be modified by excluding the  $S=3$  scale, and replacing (12) by expression  $B^{(S)} = \bar{R}m^{(S)} / \bar{R}m^{(5)}$ .

Further  $B^{(5)} = 1$ , and the lookup table should be modified. The advantages of LSDA can be exploited in a wide range of imaging systems and image processing tasks, because of its low sensitivity to the corruption factors such as a high-level noise.

## 6. ACKNOWLEDGEMENT

The research is carried out under financial support of Ministry of Education & Science of Russian Federation.

## REFERENCES

- [1] Chen C., Hwang R and Chen Y. "A passive auto-focus camera control system," Applied Soft Computing, 10, 296-303, (2010).
- [2] Bezzubik V.V., Belashenkov N.R., Ustinov S.N., "Optimization of algorithms for autofocusing a digital microscope," Journal of Optical Technology, 76(10), 603-608, (2009).
- [3] Albu F., Poenaru V. and Drimbarean A. "Autofocus method," US Patent 8508652 B2 (2013).
- [4] Krotkov E. "Focusing," International Journal of Computer Vision, 1(3), 223-237, (1987).
- [5] Crespo D., Quiroga J.A. and Gomez-Pedrero J.A. "Design of asynchronous phase detection algorithms optimized for wide frequency response," Applied Optics, 45(17), 4037-4045, (2006).
- [6] Zhu X., Cohen S., Shiller S. and Milanfar P. "Estimating spatially varying defocus blur from a single image," IEEE Transaction on Image Processing, 22(12), 4879-4891, (2013).
- [7] Elder J.H. and Zucker S.W. "Local scale control for edge detection and blur estimation," IEEE Transactions on PAMI, 20(7), 699-716, (1998).
- [8] Zhuo S. and Sim T. "Defocus map estimation from a single image," Pattern Recognition 44, 1852-1858, (2011).
- [9] Bae S. and Durand F. "Defocus magnification," Eurographics, 26(3), (2007).
- [10] Burge J. and Geiser S. "Optimal defocus estimation in individual natural images," PNAS, 108(40), 16849-16854, (2011).
- [11] Bezzubik V., Belashenkov N. and Vdovin G. "Digital deblurring based on linear-scale differential analysis", Proc. of SPIE, 9217, 92170A-1-92170A-8, (2014).
- [12] Voorhees H. and Poggio T. "Detecting textons and texture boundaries in natural images," Proc. ICCV, 250-258, (1987).